European Heart Journal Advance Access published December 14, 2010

European Heart Journal
doi:10.1093/eurheartj/ehq443

CLINICAL RESEARCH

Impaired myocardial perfusion reserve and fibrosis in Friedreich ataxia: a mitochondrial cardiomyopathy with metabolic syndrome

Subha V. Raman[1]*, Kavita Phatak[1], J. Chad Hoyle[1], Michael L. Pennell[1], Beth McCarthy[1], Tam Tran[1], Thomas W. Prior[1], John W. Olesik[1], Anthony Lutton[1], Chelsea Rankin[2], John T. Kissel[1], and Roula al-Dahhak[2]

[1]The Ohio State University, 473 W. 12th Ave, Suite 200, Columbus, OH 43210, USA; and [2]Nationwide Children's Hospital, Columbus, OH, USA

Received 22 July 2010; revised 24 September 2010; accepted 27 October 2010

Aims Cardiomyopathy produces significant mortality in patients with Friedreich ataxia (FA), a genetic disorder that produces intra-mitochondrial iron accumulation. We sought to test the hypothesis that abnormal myocardial perfusion reserve and fibrosis represent early manifestations of cardiomyopathy.

Methods and results Twenty-six patients with genetically proven FA ages 36 ± 12 years without cardiomyopathy and eight controls underwent cardiac magnetic resonance with adenosine. Precontrast imaging for myocardial iron estimation was performed. Myocardial perfusion reserve index (MPRI) was quantified using the normalized upslope of myocardial enhancement during vasodilator stress vs. rest. Left ventricular (LV) mass and volumes were computed from short-axis cine images. Serologies included lipids, and platelets were isolated for iron quantification using inductively coupled plasma mass spectrometry. Left ventricular ejection fraction and mass averaged 64.1 ± 8.3% and 62.7 ± 16.7 g/m^2, respectively, indicating preserved systolic function and absence of significant hypertrophy. Myocardial perfusion reserve index quantification revealed significantly lower endocardial-to-epicardial perfusion reserve in patients vs. controls (0.80 ± 0.18 vs. 1.22 ± 0.36, $P = 0.01$). Lower MPRI was predicted by increased number of metabolic syndrome (met-S) features ($P < 0.01$). Worse concentric remodelling occurred with increased GAA repeat length ($r = 0.64$, $P < 0.001$). Peripheral platelet iron measurement showed no distinction between patients and controls (5.4 ± 8.5 × 10^{-7} vs. 5.5 ± 2.9 × 10^{-7} ng/platelet, $P = 0.88$), nor did myocardial T2* measures.

Conclusions Patients with FA have abnormal myocardial perfusion reserve that parallels met-S severity. Impaired perfusion reserve and fibrosis occur in the absence of significant hypertrophy and prior to clinical heart failure, providing potential therapeutic targets for stage B cardiomyopathy in FA and related myocardial diseases.

Keywords Cardiomyopathy • Microcirculation • Magnetic resonance imaging • Metabolic syndrome

Introduction

Cardiac mortality is high in patients with Friedreich ataxia (FA), a genetic disorder whose major manifestations are neurological and myocardial disease. Over half of all FA patients have cardiomyopathy, classically marked by left ventricular hypertrophy (LVH), and many of these patients die of cardiac arrhythmia or congestive heart failure.[1] Historically, detection of cardiomyopathy in FA has relied on non-specific electrocardiographic abnormalities and recognition of LVH by non-invasive imaging.[2,3] Friedreich ataxia is an autosomal recessive disorder with an incidence of 1 in 30 000–50 000[4,5] caused in the majority of cases by expansion of DNA triplet repeats (GAA) in the first intron at the end of exon 1 of the frataxin gene (FRDA) on chromosome 9 leading to suppression of frataxin gene expression; rare cases (4–6%) result from point mutations.[6] The resulting defect in FA is a deficiency of the inner mitochondrial membrane protein frataxin,[6] which leads to mitochondrial iron accumulation in cardiomyocytes.[6,7]

* Corresponding author. Tel: +1 614 293 8963, Fax: +1 614 293 5614, Email: raman.1@osu.edu

Additionally, frataxin deficiency leads to increased sensitivity to oxidative stress and respiratory chain defects in cardiac and central and peripheral nervous system tissues.[5]

Several reports have suggested that idebenone, a short-chain analogue of coenzyme Q10, may slow the onset and progression of FA-associated cardiomyopathy.[3,8–10] Idebenone acts as an antioxidant via potent free radical scavenging. However, clinical trials have shown inconsistent efficacy in protecting the FA heart, even if instituted before the onset of LVH.[9,11,12] Thus, it would be useful to identify features of subclinical cardiomyopathy in FA, which too often goes unrecognized until the disease is advanced, that may serve as novel therapeutic targets. We hypothesized that impaired myocardial perfusion reserve, fibrosis, and iron overload represent early manifestations of cardiomyopathy prior to LVH that can be detected with cardiac magnetic resonance (CMR). Furthermore, we hypothesized that peripheral platelet iron levels would be elevated in patients with FA, offering a serological surrogate of disease.

Methods

Subjects

Friedreich ataxia patients with no known history of cardiomyopathy (heart failure, arrhythmias, or systolic dysfunction) were identified from the ataxia clinics of the Ohio State University and Nationwide Children's Hospital, as well as through advertising via the Friedreich's Ataxia Research Alliance. Control subjects of similar age were recruited from volunteers aware of the protocol, without cardiovascular disease, diabetes, or hypertension. Individuals with abnormal renal function (calculated glomerular filtration rate $\leq$ 30 mL/min/m^2), allergy to gadolinium-based contrast or adenosine, severe claustrophobia, ferromagnetic foreign body, non-MR compatible aneurysm clip, pacemaker, defibrillator, or other active implant were excluded from enrolment. All participants provided written informed consent to participate in this Institutional Review Board-approved investigation.

Neurologic functional assessment was performed using the Freidreich Ataxia Rating Scale (FARS).[13–15] Baseline clinical characteristics were recorded including age, gender, height, weight, blood pressure, history of cardiac symptoms, pertinent medical history, and medications. All patients had undergone echocardiography within the prior year indicating normal LV function. Laboratory examination included fasting lipid profile and glucose measurements. Resting electrocardiography (ECG) was performed in all subjects. Total number of metabolic syndrome (met-S) features among the following were recorded: (i) triglyceride level $\geq$150 mg/dL, (ii) HDL $<$40 mg/dL for men or $<$50 mg/dL for women, (iii) fasting blood glucose $\geq$100 mg/dL, (iv) elevated blood pressure (systolic $\geq$130 or diastolic $\geq$85 mmHg, or treatment for hypertension), and (v) body mass index $\geq$25 kg/m^2 as a surrogate for waist circumference in this mostly wheelchair-bound Caucasian population.[16,17]

Genetic testing

Genetic testing used either commercial laboratories or in-house assay. For the latter, genomic DNA was isolated from whole blood leucocytes and 15 μg was digested for 5 h at 65°C with BsiHKAI enzyme (New England Biolabs). The digested DNA was size-fractionated by 0.8% agarose gel electrophoresis. The gels were blotted onto nylon membranes, as described by Southern, and hybridized with a ^{32}P-radiolabelled 463-bp genomic fragment containing the FRDA exon 1.[18] Blots were initially washed in 2× saline sodium citrate (SSC) and 0.5% sodium dodecyl sulfate (SDS) at 42°C for 30 min, followed by a second wash for 30 min at 42°C in 1×SSC and 0.5% SDS. Finally, blots were washed twice at 60°C in a solution of 0.5 × SSC and 0.4% SDS. Autoradiographs with intensifying screens were processed at −70°C for 1–3 days. The BsiHKAI enzyme produces a 2.4 kb target fragment.

Cardiac magnetic resonance protocol

All subjects underwent comprehensive CMR examination using a 1.5 T scanner (Siemens MAGNETOM Avanto), 12-channel phased array surface cardiac coil and the following imaging protocol:

(i) Myocardial iron measurement, using an ECG-triggered segmented, multiple-echo, gradient-echo acquisition with echo times (TE) of 1.22, 2.64, 4.59, 7.56, 11.1, 15.0, 18.9, 22.8, and 26.7 ms.

(ii) Vasodilator stress with intravenous infusion of adenosine 140 μg/kg, with simultaneous ECG and blood pressure monitoring. After 3 min, stress perfusion images were acquired with administration of 0.075 mmol/kg gadolinium-diethylenetriamine penta-acetic acid (DTPA) in the other arm with ongoing administration of adenosine during perfusion scan acquisition.[19] Perfusion imaging in three short-axis planes and one long-axis plane employed a hybrid gradient echo–echo planar (GRE-EPI) technique with adaptive temporal sensitivity encoding (TSENSE) with 40 acquisitions per plane. Once stress perfusion was completed (1 min), the adenosine infusion was terminated.

(iii) Multi-plane (horizontal long-axis, contiguous short-axis, vertical long-axis, and three-chamber long-axis) cine imaging for LV size and function measurement using a steady-state free precession pulse sequence with the following scan parameters: slice thickness of 8 mm, interslice gap for short-axis imaging of 2 mm, average in-plane spatial resolution of 1.5 mm.

(iv) Fifteen minutes after stress perfusion was completed, resting perfusion images were obtained in the identical planes as during stress using an additional 0.075 mmol/kg intravenous gadolinium-DTPA.

(v) Multi-plane late gadolinium enhancement (LGE) imaging was obtained for visualization of myocardial fibrosis using a fast gradient-echo inversion-recovery prepped technique with appropriate inversion time selection.[20] Late gadolinium enhancement imaging used a slice thickness of 8 mm and in-plane spatial resolution of 1.5 mm.

Image analysis

Left ventricular mass and ejection fraction (EF) were measured from contiguous short-axis cine images using endocardial and epicardial contours drawn at end-systole and end-diastole, where the volumes from each short-axis slice are summed to obtain global measures[21]. Left atrial area was measured at the end of ventricular systole in the horizontal long-axis plane. All volume, mass, and area measurements are reported indexed to body surface area. Relative wall thickness (RWT) was measured at the end of ventricular diastole in a mid-short-axis slice as follows: RWT = (septal thickness + lateral wall thickness)/LV internal dimension.[22] Left ventricular hypertrophy was present if LV mass indexed to body surface area exceeded the 95% percentile based on gender ($>$91 g/m^2 for males or $>$77 g/m^2 for females).[21] Concentric remodelling was present if RWT was $\geq$0.44 for males or $\geq$0.45 for females.[22] Using the images from all nine TEs in the multi-echo gradient-echo acquisition, myocardial T2* was computed using mono-exponential decay curve fitting and previously validated post-processing software.[23]

Quantification of myocardial perfusion was performed using semi-automatic delineation of endocardial and epicardial LV borders throughout the phases of first-pass perfusion with respiratory motion correction as needed (CMRTools, London). Perfusion analysis was performed on images obtained in a mid-short-axis slice, with a thickness of 10 mm. Rest and stress myocardial perfusion slopes were derived using Fermi-fitting of signal intensity vs. time and normalized to the LV blood pool slope as well as the heart rate. A Myocardial perfusion reserve index (MPRI) was calculated for each subject, defined as the ratio of stress to rest, normalized myocardial perfusion slope.[24] Late gadolinium enhancement images were visually inspected using a standardized 17-segment myocardial model[25] as demonstrating either a presence (1) or absence (0) of hyper-enhancement.

Platelet iron quantification protocol

Platelet-rich plasma was isolated from blood samples, to which prostaglandin E1 was added. Pellets were flash frozen and subsequently thawed for batch processing and re-suspended with Tyrodes solution at pH 7.4, and platelets were counted with a Coulter counter. The total iron amount was measured with inductively coupled plasma mass spectrometry (ICP-MS). Each aliquot of 0.2 mL of aqueous solution containing suspended platelets was diluted to 10 mL in 2% concentrated nitric acid. Cobalt was added to each sample and standard at a fixed concentration and used as an internal standard. Samples were analysed with a ThermoFinnigan Element 2 ICP-sector field-MS[26] used in medium resolution ($R = 4000$) to resolve spectral overlaps so that iron was measured as its major isotope with in-house developed method parameters. Tyrodes solution was assessed separately and found to be free of iron. In one aliquot of one sample, a known amount (spike) of Fe was added and the recovery was within 6% of the expected value, showing that the sensitivity (slope/concentration) was the same in the sample and standards. After the platelets underwent digestion, iron levels were serially measured until they reached a plateau, ensuring that digestion of the mitochondrial membrane was complete.

Statistical analysis

Continuous variables are expressed as mean ± standard deviation (SD). Patients and controls were compared using Fisher's exact test for binary outcomes and unequal variance *t*-tests for continuous outcomes. We used a multiple linear regression model for MPRI containing metabolic abnormalities (two levels: 0 or 1 vs. 2 or more met-S factors) as a predictor. Confounding variables (age, gender, and FARS score) were selected using a forward selection methodology; confounders were sequentially added if their inclusion changed the estimated effect of metabolic abnormalities on MPRI by 10% or more; a *P*-value of <0.05 was deemed significant. We also used multiple linear regression to examine the relationship between MPRI and the number of met-S factors, adjusting for the same confounders selected in the model treating metabolic abnormalities as a binary variable. The relationship between the size of the GAA expansion on the smaller allele and the RWT was examined using simple linear regression. Data were analysed using Stata/SE 8.1 (College Station, TX, USA), SAS version 9.2 and JMP version 8 (SAS Inc., Cary, NC, USA).

Results

Twenty-six patients with FA aged 18–57 years and eight controls aged 22–44 years completed the study protocol between January 2008 and June 2010. Two patients' blood could not be processed for genotyping, though neurologic phenotype in both cases was classic for FA. In the remaining 24 patients, genetic testing demonstrated GAA expansions ranging from 41 to 1500 (*Figure 1*). Two had point mutations: one with a T- to C- in the frataxin gene (L106S)[27] and another with C- to T- replacement (R165C).[28] All subjects were Caucasian, including three of Middle Eastern origin. None reported a history of hypertension or diabetes. Four FA patients were on idebenone, and one was on niacin for hypertriglyceridaemia. Demographic and other variables are summarized in *Table 1*. The mean FARS score was 72 ± 30, and the median disease stage was 5 (IQR 4–5) on a 0–6 scale, with 5 representing confinement to but ability to navigate a wheelchair. Only 6 FA patients' ECGs had no abnormality; 16 had non-specific ST-T-wave abnormalities and the remaining 4 met ECG criteria for LVH with re-polarization abnormality.

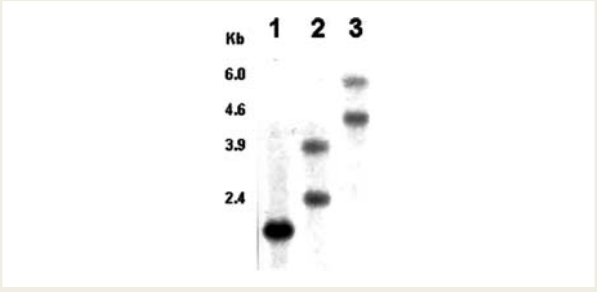

Figure 1 Southern blot analysis shows no GAA expansion in a normal control (lane 1), 160 and 500 repeats in an affected control (lane 2), and ~733 and 1200 repeats in Friedreich ataxia patient 28 (lane 3).

Table 1 Demographic characteristics and cardiac measurements by magnetic resonance imaging in patients with Friedreich ataxia vs. controls

	Patients (*N* = 26)	Controls (*N* = 8)	*P*-value
Age (years)	35.8 ± 11.7	31.4 ± 7.0	0.20
Male gender, *n* (%)	8 (31)	4 (50)	0.41
BMI (kg/m^2)	24.5 ± 6.9	22.6 ± 3.4	0.30
LV ejection fraction (%)	64.1 ± 8.3	61.7 ± 6.9	0.42
Left atrial area index (cm^2/m^2)	9.6 ± 2.8	9.6 ± 3.7	0.98
LV mass index (g/m^2)	61.7 ± 16.7	48.4 ± 7.0	0.003
LV end-diastolic volume index (mL/m^2)	54.6 ± 13.4	70.2 ± 19.4	0.06
LV end-systolic volume index (mL/m^2)	19.6 ± 7.3	26.8 ± 9.4	0.08
Relative wall thickness	0.40 ± 0.09	0.28 ± 0.07	0.001
MPRI	0.80 ± 0.18[a]	1.22 ± 0.36	0.012

[a]*N* = 25.

Left ventricular structure and function

Left ventricular volumes, mass, EF, and left atrial area were similar in FA patients and controls, with a trend towards smaller LV volumes in patients vs. controls (*Table 1*). Only four FA patients met LV mass criteria for LVH. Relative wall thickness was significantly higher in patients compared with controls (0.40 ± 0.09 vs. 0.28 ± 0.07, $P = 0.001$), with eight patients (31%) and no controls meeting criteria for concentric remodelling ($P = 0.15$). Increased concentric remodelling occurred with greater GAA triplet expansion length ($r = 0.64$, $P < 0.001$, *Figure 2*). This relationship was even stronger ($r = 0.78$, $P < 0.0001$) following omission of an outlier in the data (RWT = 0.68, minGAA = 160).

Comparison with available echocardiography data

Prior echocardiograms were reviewed where available, as summarized in *Table 2*. Many patients had undergone echocardiography remotely (>12 months) prior to CMR examination, precluding reliable comparison of LV measurements between modalities. In two, the transthoracic acoustic window was limited precluding accurate M-mode measurement; contrast was not administered for either procedure.

Myocardial perfusion reserve, fibrosis, and T2*

Quantification of the ratio of endocardial to epicardial MPRI was feasible in all but one subject (FA20: excessive motion), and revealed significant impairment in patients compared with controls [0.80 ± 0.18 vs. 1.22 ± 0.36, respectively (*Figure 3*, $P = 0.01$)]. Adjustment for the neurologic score affected the estimated difference by <10%. Fifteen FA subjects (58%) showed myocardial hyper-enhancement on LGE imaging, not present in any controls ($P = 0.0045$). The pattern, when present, was typically mild mid-myocardial fibrosis of the interventricular septum (*Figure 4*). Friedreich ataxia patients' myocardial T2* averaged 28.5 ± 5.0 ms (normal >20 ms), indicating lack of measurable iron aggregates by this technique.

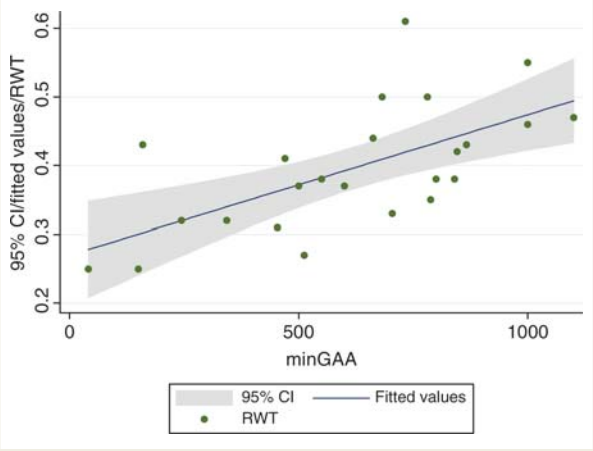

Figure 2 Size of the GAA expansion on the smaller allele (minGAA) vs. relative wall thickness (RWT) in patients shows increased concentric remodelling with increased pathologic GAA expansion ($r = 0.64$, $P < 0.001$).

Table 2 Cardiac magnetic resonance and echocardiography measures

Subject No.	CMR-LVMI	CMR-RWT	Echo-RWT	Interval (months)
1	67.6	0.38	0.30	18
2	61.6	0.42	0.46	<1
5	39.3	0.32	NA1	6
6	55.3	0.33	0.24	40
7	61.6	0.38	0.36	18
8	56.0	0.43	0.34	26
9	68.0	0.41	NA2	NA
10	99.0	0.47	NA2	1
11	54.0	0.25	NA2	NA
12	73.0	0.38	0.40	10
13	53.0	0.44	0.35	18
14	41.0	0.27	0.48	5
15	56.7	0.32	NA2	NA
16	41.4	0.43	NA2	NA
17	35.2	0.34	0.36	12
18	50.3	0.35	0.44	8
19	83.0	0.5	NA	NA
20	63.2	0.37	0.43	2
21	41.1	0.46	0.48	2
22	92.9	0.5	NA	NA
23	77.6	0.31	NA	NA
24	89.8	0.55	0.87	20
25	64.9	0.37	NA1	9
26	55.1	0.43	NA2	NA2
27	60.0	0.25	0.42	19
28	65.0	0.61	NA2	NA2

NA1, not available due to inadequate M-mode images for measurement; NA2, echocardiogram not available for review; LVMI, left ventricular mass index.

Serologies

Measurement of iron in isolated peripheral blood showed no detectable difference in FA patients vs. controls ($5.4 \pm 8.5 \times 10^{-7}$ vs. $5.5 \pm 2.9 \times 10^{-7}$ ng/platelet, $P = 0.880$). However, FA patients had significant lipid abnormalities: HDL averaged 39.9 ± 18.0, triglycerides 170.3 ± 344.1, LDL 102.7 ± 34.4, and total cholesterol 166.9 ± 44.4 mg/dL. Using the criteria for serologies, blood pressure and body size defined above, all but four FA patients had at least 1 met-S factor (median 1.5, IQR 1–3), and eight (31%) had 3 or more. Increasing number of met-S features predicted a worse MPRI (*Figure 5*); mean MPRI in patients with 0 or 1 met-S factor was significantly higher compared with those with 2 or more (unadjusted: −0.171, $P = 0.018$); adjustments for age, FARS score, or gender changed the estimated difference by <10%.

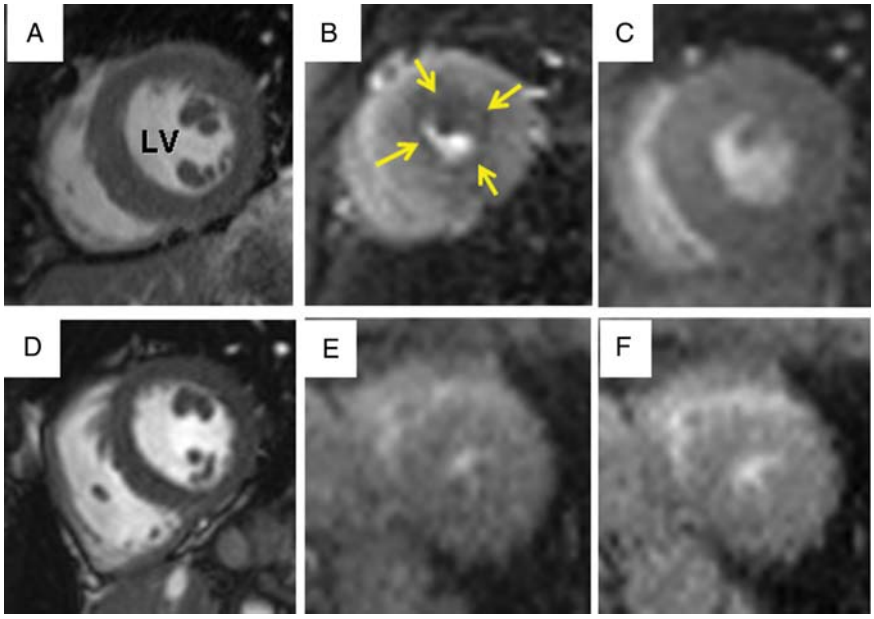

Figure 3 Cardiac magnetic resonance end-diastolic images of the left ventricle (LV) in cross-section (*A* and *D*), stress perfusion (*B* and *E*), and rest perfusion (*C* and *F*) are shown from two 33-year-old patients with Friedreich ataxia. The first (*A*–*C*) has concentric remodelling (RWT 0.46) and impaired myocardial perfusion reserve (*B*, arrows; MPRI 0.7) compared with the second (*D*–*F*) who has normal RWT (0.38) and normal perfusion reserve (MPRI 1.1). RWT, relative wall thickness; MPRI, myocardial perfusion reserve index.

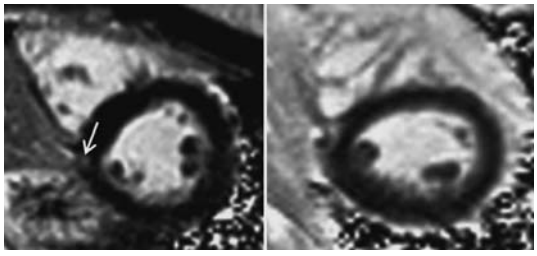

Figure 4 Late gadolinium enhancement images demonstrate mid-myocardial fibrosis at the inferior RV–LV junction in one Friedreich ataxia patient (left, arrow) compared with the similar acquisition in a late gadolinium enhancement-negative Friedreich ataxia patient (right).

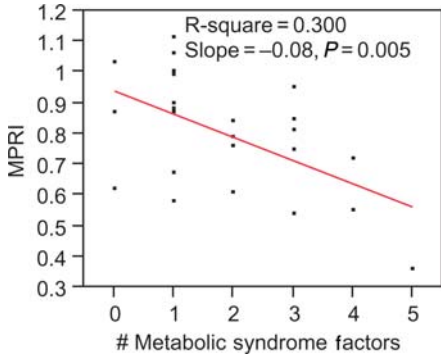

Figure 5 Linear regression of endocardial to epicardial myocardial perfusion reserve index (MPRI) vs. number of metabolic syndrome factors (0 through 5) demonstrates worse perfusion reserve with increased number of met-S risk factors.

Discussion

In this study, we identified impaired myocardial perfusion reserve and myocardial fibrosis in patients with FA without clinically evident cardiomyopathy. We also found evidence of concentric remodelling that worsened with GAA repeat length. This occurred in the absence of significant LV hypertrophy, which is classically thought to represent the typical cardiac morphology of FA-associated cardiomyopathy. The impaired myocardial perfusion reserve in FA occurred against a backdrop of features consistent with the met-S, and increased number of met-S features worsened perfusion reserve impairment after adjusting for age.

Mitochondrial function is essential for normal flow-mediated vasodilatation of the myocardial microcirculation.[29] Our work suggests that microvascular disease and fibrosis are functional and structural sequelae of impaired mitochondrial function; the latter, in turn, constitutes the genetically determined abnormality in FA as a consequence of a specific mutation in the mitochondrial protein frataxin. *Figure 6* presents a possible mechanistic framework linking the met-S that results from insulin dyscrasia and skeletal lipogenesis,[30] recent evidence that indicates that the met-S itself affects capillary density,[31] and frataxin's function in keeping iron from accumulating in endothelial cell mitochondria[32] to the

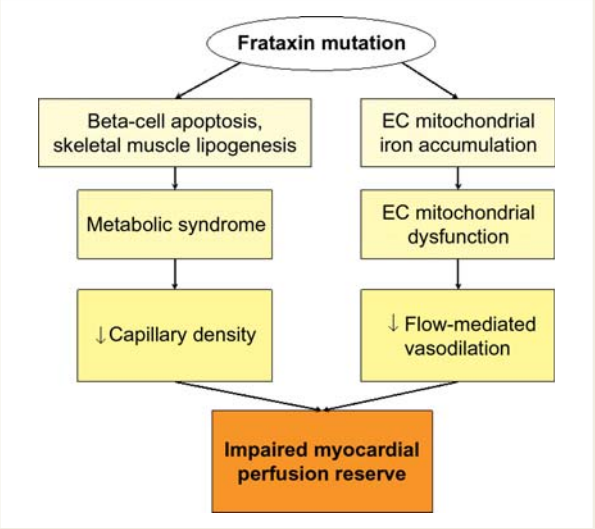

Figure 6 Frataxin deficiency affects insulin production as well as skeletal lipogenesis, both potentially contributing to metabolic syndrome that may itself affect capillary density. In conjunction with a possible direct effect on endothelial cells (EC), these effects may act synergistically to limit myocardial perfusion reserve.

impaired myocardial perfusion reserve in FA. Mitochondrial dysfunction is increasingly recognized as the next potential treatment target in cardiomyopathy due to various causes,[33] underscoring the value of studying a well-defined genetic disease to impact the broader population as advocated in a recent NIH Research Agenda statement.[34] Our identification of impaired perfusion reserve and fibrosis as signatures of myocardial disease in FA prior to overt clinical abnormalities and in conjunction with metabolic dyscrasias suggests that these may serve as new treatment targets to prevent heart failure in FA patients. Further, the correlation between impaired perfusion reserve and the met-S in a genetic disorder of mitochondrial dysfunction may hold promise in developing novel therapeutic approaches for millions of individuals with the met-S.

We did not detect a difference between myocardial T2* in FA patients vs. controls. While iron may accumulate within mitochondria in FA patients' cardiomyocytes, the intra-mitochondrial iron particles are relatively isolated compared with the large iron aggregates seen in transfusion-associated myocardial iron overload that produce local changes in magnetic field susceptibility, which are measurable as shortened T2* values.

Platelet iron content would seem to be an appealing serologic biomarker of disease, given the high concentration of mitochondria in this blood component. However, ICP-MS did not detect a difference. One possible explanation is that frataxin shows tissue-specific mosaicism in development[35] and may not be present in megakaryocytes. Another reason may be that a high platelet turnover may prevent iron accumulation. Notably, bleeding diathesis or other reports of platelet dysfunction have not been described in FA, suggesting that platelets may not be affected by frataxin deficiency.

Limitations of this work include a relatively small sample size imposed by the rarity of the genetic disorder. However, we achieved sufficient statistical power given the magnitude of the differences detected. Nonetheless, multi-centre studies are needed to confirm our findings in a larger FA population and to include a therapeutic intervention targeting these findings of subclinical myocardial disease. Many of the GAA expansions were very mosaic, which could affect the repeat size accuracy, and the expanded allele in lymphocytes may not always be equivalent to the size in the affected tissue; nonetheless, GAA repeat length in peripheral lymphocytes performed well in predicting the severity of cardiac remodelling.

There are several implications for early detection and treatment to prevent the progression of cardiomyopathy in FA. First, impaired mobility in many FA patients with advancing neurological disease may allow subclinical cardiomyopathy to be present in the absence of the exertional symptoms that occur in ambulatory patients with myocardial disease. Our results motivate further studies to better define the role of CMR to detect subclinical myocardial ischaemia and fibrosis, which might otherwise go untreated, with agents such as angiotensin-converting enzyme-inhibitors vs. screening with serial echocardiography that may require more careful attention to subtle structural abnormalities such as concentric remodelling. Angiotensin-converting enzyme-inhibitor and other medical therapies are well established in the setting of 'stage B cardiomyopathy'—structural disease in the absence of clinical symptoms of heart failure[36]. The guidelines do not, however, recognize impaired perfusion reserve and fibrosis by CMR as evidence of structural heart disease to prompt institution of cardioprotective therapies. Randomized trials are warranted, given our findings of impaired perfusion reserve and fibrosis prior to heart failure, which also include direct comparison with standardized echocardiography with appropriate tissue Doppler acquisitions, previously shown to be abnormal in proportion to GAA expansion severity[37]. Recognition that metabolic abnormalities occur in conjunction with reduced sub-endocardial perfusion reserve and fibrosis warrants inclusion of therapies such as lipid-lowering agents to attenuate myocardial disease progression. Although clinical trials have yet to yield major advances in treating either neurologic or cardiac disease in FA, identification of subclinical structural and functional changes with mechanistic correlates to the underlying mitochondrial dysfunction could guide institution of available cardioprotective therapies for FA patients in the short-term while novel therapies are developed.

In summary, patients with FA have abnormal myocardial perfusion reserve and fibrosis in the absence of overt hypertrophy and contractile dysfunction, which appear to precede clinically apparent cardiomyopathy. Further investigation of these findings may yield novel therapeutic targets for both this population as well as patients at risk of related cardiomyopathies.

Acknowledgements

The authors thank David R. Lynch, MD, PhD and Jennifer Farmer, MS, CGC of FARA for their support and guidance, and the inspiring individuals with FA who participated in this study.

Funding

This work was supported by a Kyle Bryant Translational Research Award jointly funded by Ride Ataxia II, the Friedreich's Ataxia Research Alliance (FARA), and the National Ataxia Foundation. Statistical support was provided via UL1RR025755.

Conflict of interest: S.V.R. receives research support from Siemens.

References

1. Ropper AH, Samuels MA. *Adams and Victor's Principles of Neurology*, 9th Edition, USA: The McGraw-Hill Companies, Inc., 2009.
2. Child JS, Perloff JK, Bach PM, Wolfe AD, Perlman S, Kark RA. Cardiac involvement in Friedreich's ataxia: a clinical study of 75 patients. *J Am Coll Cardiol*. 1986;**7**: 1370–1378.
3. Meyer C, Schmid G, Gorlitz S, Ernst M, Wilkens C, Wilhelms I, Kraus PH, Bauer P, Tomiuk J, Przuntek H, Mugge A, Schols L. Cardiomyopathy in Friedreich's ataxia-assessment by cardiac MRI. *Mov Disord* 2007;**22**:1615–1622.
4. Delatycki MB, Williamson R, Forrest SM. Friedreich ataxia: an overview. *J Med Genet.* 2000;**37**:1–8.
5. Pandolfo M. Friedreich ataxia. *Arch Neurol* 2008;**65**:1296–1303.
6. Campuzano V, Montermini L, Molto MD, Pianese L, Cossee M, Cavalcanti F, Monros E, Rodius F, Duclos F, Monticelli A, Zara F, Canizares J, Koutnikova H, Bidichandani SI, Gellera C, Brice A, Trouillas P, De Michele G, Filla A, De Frutos R, Palau F, Patel PI, Di Donato S, Mandel JL, Cocozza S, Koenig M, Pandolfo M. Friedreich's ataxia: autosomal recessive disease caused by an intronic GAA triplet repeat expansion. *Science* 1996;**271**:1423–1427.
7. Bradley JL, Blake JC, Chamberlain S, Thomas PK, Cooper JM, Schapira AH. Clinical, biochemical and molecular genetic correlations in Friedreich's ataxia. *Hum Mol Genet* 2000;**9**:275–282.
8. Di Prospero NA, Sumner CJ, Penzak SR, Ravina B, Fischbeck KH, Taylor JP. Safety, tolerability, and pharmacokinetics of high-dose idebenone in patients with Friedreich ataxia. *Arch Neurol* 2007;**64**:803–808.
9. Schols L, Vorgerd M, Schillings M, Skipka G, Zange J. Idebenone in patients with Friedreich ataxia. *Neurosci Lett* 2001;**306**:169–172.
10. Seznec H, Simon D, Monassier L, Criqui-Filipe P, Gansmuller A, Rustin P, Koenig M, Puccio H. Idebenone delays the onset of cardiac functional alteration without correction of Fe-S enzymes deficit in a mouse model for Friedreich ataxia. *Hum Mol Genet* 2004;**13**:1017–1024.
11. Ribai P, Pousset F, Tanguy ML, Rivaud-Pechoux S, Le Ber I, Gasparini F, Charles P, Beraud AS, Schmitt M, Koenig M, Mallet A, Brice A, Durr A. Neurological, cardiological, and oculomotor progression in 104 patients with Friedreich ataxia during long-term follow-up. *Arch Neurol* 2007;**64**:558–564.
12. Rinaldi C, Tucci T, Maione S, Giunta A, De Michele G, Filla A. Low-dose idebenone treatment in Friedreich's ataxia with and without cardiac hypertrophy. *J Neurol* 2009;**256**:1434–1437.
13. Delatycki MB. Evaluating the progression of Friedreich ataxia and its treatment. *J Neurol* 2009;**256** (Suppl. 1):36–41.
14. Subramony SH, May W, Lynch D, Gomez C, Fischbeck K, Hallett M, Taylor P, Wilson R, Ashizawa T. Measuring Friedreich ataxia: interrater reliability of a neurologic rating scale. *Neurology* 2005;**64**:1261–1262.
15. Lynch DR, Farmer JM, Tsou AY, Perlman S, Subramony SH, Gomez CM, Ashizawa T, Wilmot GR, Wilson RB, Balcer LJ. Measuring Friedreich ataxia: complementary features of examination and performance measures. *Neurology* 2006; **66**:1711–1716.
16. Alberti KGMM, Eckel RH, Grundy SM, Zimmet PZ, Cleeman JI, Donato KA, Fruchart J-C, James WPT, Loria CM, Smith SC Jr. Harmonizing the metabolic syndrome: a joint interim statement of the International Diabetes Federation Task Force on Epidemiology and Prevention; National Heart, Lung, and Blood Institute; American Heart Association; World Heart Federation; International Atherosclerosis Society; and International Association for the Study of Obesity. *Circulation* 2009;**120**:1640–1645.
17. Calle EE, Thun MJ, Petrelli JM, Rodriguez C, Heath CW Jr. Body-mass index and mortality in a prospective cohort of U.S. adults. *N Engl J Med* 1999;**341**: 1097–1105.
18. Durr A, Cossee M, Agid Y, Campuzano V, Mignard C, Penet C, Mandel JL, Brice A, Koenig M. Clinical and genetic abnormalities in patients with Friedreich's ataxia. *N Engl J Med* 1996;**335**:1169–1175.
19. Klem I, Heitner JF, Shah DJ, Sketch MH Jr, Behar V, Weinsaft J, Cawley P, Parker M, Elliott M, Judd RM, Kim RJ. Improved detection of coronary artery disease by stress perfusion cardiovascular magnetic resonance with the use of delayed enhancement infarction imaging. *J Am Coll Cardiol* 2006;**47**:1630–1638.
20. Kim RJ, Shah DJ, Judd RM. How we perform delayed enhancement imaging. *J Cardiovasc Magn Reson* 2003;**5**:505–514.
21. Maceira AM, Prasad SK, Khan M, Pennell DJ. Normalized left ventricular systolic and diastolic function by steady state free precession cardiovascular magnetic resonance. *J Cardiovasc Magn Reson* 2006;**8**:417–426.
22. Velagaleti RS, Gona P, Levy D, Aragam J, Larson MG, Tofler GH, Lieb W, Wang TJ, Benjamin EJ, Vasan RS. Relations of biomarkers representing distinct biological pathways to left ventricular geometry. *Circulation* 2008;**118**: 2252–2258, 2255p following 2258.
23. Raman SV, Simonetti OP, Cataland SR, Kraut EH. Myocardial ischemia and right ventricular dysfunction in adult patients with sickle cell disease. *Haematologica* 2006;**91**:1329–1335.
24. Cook SC, Ferketich AK, Raman SV. Myocardial ischemia in asymptomatic adults with repaired aortic coarctation. *Int J Cardiol* 2009;**133**:95–101.
25. Cerqueira MD, Weissman NJ, Dilsizian V, Jacobs AK, Kaul S, Laskey WK, Pennell DJ, Rumberger JA, Ryan T, Verani MS. Standardized myocardial segmentation and nomenclature for tomographic imaging of the heart: a statement for healthcare professionals from the Cardiac Imaging Committee of the Council on Clinical Cardiology of the American Heart Association. *Circulation* 2002;**105**: 539–542.
26. Jakubowski N, Moens L, Vanhaecke F. Sector field mass spectrometers in ICP-MS. *Spectrochim Acta Part B At Spectrosc* 1998;**53**:1739–1763.
27. Bartolo C, Mendell JR, Prior TW. Identification of a missense mutation in a Friedreich's ataxia patient: implications for diagnosis and carrier studies. *Am J Med Genet* 1998;**79**:396–399.
28. Forrest SM, Knight M, Delatycki MB, Paris D, Williamson R, King J, Yeung L, Nassif N, Nicholson GA. The correlation of clinical phenotype in Friedreich ataxia with the site of point mutations in the FRDA gene. *Neurogenetics* 1998;**1**:253–257.
29. Liu Y, Zhao H, Li H, Kalyanaraman B, Nicolosi AC, Gutterman DD. Mitochondrial sources of H2O2 generation play a key role in flow-mediated dilation in human coronary resistance arteries. *Circ Res* 2003;**93**:573–580.
30. Coppola G, Marmolino D, Lu D, Wang Q, Cnop M, Rai M, Acquaviva F, Cocozza S, Pandolfo M, Geschwind DH. Functional genomic analysis of frataxin deficiency reveals tissue-specific alterations and identifies the PPARgamma pathway as a therapeutic target in Friedreich's ataxia. *Hum Mol Genet* 2009;**18**: 2452–2461.
31. Czernichow S, Greenfield JR, Galan P, Jellouli F, Safar ME, Blacher J, Hercberg S, Levy BI. Macrovascular and microvascular dysfunction in the metabolic syndrome. *Hypertens Res* 2010;**33**:293–297.
32. Carraway MS, Suliman HB, Madden MC, Piantadosi CA, Ghio AJ. Metabolic capacity regulates iron homeostasis in endothelial cells. *Free Radic Biol Med* 2006;**41**:1662–1669.
33. Ingwall JS, Weiss RG. Is the failing heart energy starved? On using chemical energy to support cardiac function. *Circ Res* 2004;**95**:135–145.
34. Collins FS. Opportunities for research and NIH. *Science* 2010;**327**:36–37.
35. Jiralerspong S, Liu Y, Montermini L, Stifani S, Pandolfo M. Frataxin shows developmentally regulated tissue-specific expression in the mouse embryo. *Neurobiol Dis* 1997;**4**:103–113.
36. Hunt SA, Abraham WT, Chin MH, Feldman AM, Francis GS, Ganiats TG, Jessup M, Konstam MA, Mancini DM, Michl K, Oates JA, Rahko PS, Silver MA, Stevenson LW, Yancy CW. Focused Update Incorporated Into the ACC/AHA 2005 Guidelines for the Diagnosis and Management of Heart Failure in Adults: A Report of the American College of Cardiology Foundation/American Heart Association Task Force on Practice Guidelines Developed in Collaboration With the International Society for Heart and Lung Transplantation. *J Am Coll Cardiol* 2009;**53**:e1–e90.
37. Dutka DP, Donnelly JE, Palka P, Lange A, Nunez DJ, Nihoyannopoulos P. Echocardiographic characterization of cardiomyopathy in Friedreich's ataxia with tissue Doppler echocardiographically derived myocardial velocity gradients. *Circulation* 2000;**102**:1276–1282.